ADVANCED STRUCTURAL SIZING METHODOLOGY

W. Jefferson Stroud and Jaroslaw Sobieszczanski-Sobieski

NASA Langley Research Center

INTRODUCTION

Aircraft having unusual and unprecedented configurations may be considered for future CTOL applications in order to meet requirements of energy efficiency, military performance, and economic viability. (See, for example, ref. 1.) In addition, new and emerging technologies such as composite structures, active controls, and laminar-flow control may find application on future aircraft with either conventional or unconventional configurations. This situation presents a challenge to perform the structural design of these future aircraft with little or no historical data base and at a reasonable cost.

A rapidly developing technology that can help engineers meet this design challenge is mathematical modeling and computerized (or automated) structural sizing. The problems and potential of this approach were outlined 5 yr ago in reference 2. Since that time, numerous advances have made computerized structural sizing even more attractive.

The purpose of this paper is to describe Langley Research Center activities aimed at developing useful computerized structural sizing technology. Four areas are considered: overall vehicle design, structural subassembly design, thermal structures, and stiffened panels. In each case, sample results are presented. Details and analytical foundations are found in the references.

COMPUTERIZED STRUCTURAL SIZING METHODOLOGY

For over a decade, Langley Research Center has performed inhouse research and sponsored grants and contracts in the area of computerized structural sizing. That work is now concentrated in the following four research areas:

(1) <u>Overall vehicle</u> - sizing work in which technology is being developed to consider the integrated effect of several disciplines - such as structures, materials, aerodynamics, propulsion, and active controls - early in the design process

(2) <u>Structural subassembly</u> - smaller scale sizing work which concentrates on structural sizing methodology for finite-element structural models

(3) <u>Thermal structures</u> - high-speed aircraft may have special design problems associated with high temperatures, and special sizing techniques are needed to handle these problems

(4) Stiffened panels - Langley has a strong analytical and experimental program aimed at the design of efficient stiffened composite panels. This report considers only a portion of the analytical stiffened panel work

Overall Vehicle Structural Sizing

Desired output.- The output of our current overall vehicle sizing codes is the static and dynamic aeroelastic characteristics of aircraft with and without active controls. We can also obtain structural mass, stiffness distribution, structural layout, and dimensions of key structural members. The goal, however, is more ambitious; we want to obtain propulsion, performance, and economic output.

Level of structural detail.- A typical finite-element model of a low-aspect-ratio supersonic aircraft used in our studies is shown in figure 1. The model shows the level of structural detail being considered. In this example, emphasis is placed on fairly detailed modeling of the wing. The fuselage and tail are modeled more simply to give adequate stiffness and dynamic characteristics.

Structural sizing approach.- The present sizing approach, together with an improved approach denoted "goal," is outlined in figure 2. In the present approach, the airframe geometry (wing planform, wing depth distribution, etc.) is assumed to be given and fixed. Because the procedure includes a static aeroelastic capability (i.e., the pressure distribution depends upon the deflected shape of the wing), iteration is often required to obtain the aerodynamic loading. That iteration is indicated by the circle with arrows connecting the block labeled "Aerodynamic Loads Analysis" with the block labeled "Structural Finite-Element Analysis." The structural elements are also sized for minimum mass. Sizing is indicated by the circle with arrows connecting the block labeled "Structural Finite-Element Analysis" with the block labeled "Sizing of Structural Elements." This sizing affects the stiffness distribution which, in turn, affects the pressure distribution. The sizing is, therefore, a multiloop iterative scheme which results in a strength-sized airframe. Then, if flutter is a problem, the structure can be stiffened with additional material, or an active control system can be employed. The final product is an airframe sized to meet strength and flutter design requirements.

The present approach is sequential. The wing is first sized for strength. During the strength sizing, wing panels are sized for minimum mass on a panel-by-panel basis. That is, no attempt is made to favorably influence the aerodynamic loading or the resulting internal load distributions. After the wing is sized for strength, additional material (or an active control system) is added to prevent flutter. To reduce computer resources, flutter sizing is carried out on a simplified finite-element model rather than on the refined model (fig. 1) used in the strength sizing procedure. A spline function technique is used to transfer sizing data from one model to another. Both the strength and flutter sizing procedures are based on nonlinear mathematical programming, which is a general purpose mathematical search technique. A complete discussion of the sizing approach, together with example applications, is presented in references 3 and 4.

In contrast with the present sequential approach, the goal is a simultaneous approach in which values of all sizing variables (dimensions of structural members, size and location of active control systems, etc.) are determined based on their effect on all the design requirements (strength, flutter, etc.). In such an approach, all sizing variables and all design requirements are considered simultaneously. The goal approach takes advantage of the interaction between the active control system, structural member size, aerodynamic loading, and wing load paths. Finally, airframe geometry is defined by variables that could be adjusted during the structural sizing process. The goal approach would provide a design that is superior to the one obtained by using the present approach.

Framework of overall vehicle sizing system.- Although the goal in the overall vehicle sizing procedure has not yet been reached, the framework for a large multidisciplinary sizing system called Integrated Synergistic Synthesis System (ISSYS) has been developed and made operational. That framework is depicted in figure 3. One key point about this system is that instead of developing an executive system to link the users to the data base (represented in fig. 3 by the entire large box below the two large arrows), we are using the Control Data Corporation computer operating system (denoted NOS) which is resident on the Control Data computers at Langley. Any modern standard time-share operating system can serve as the executive system.

Users issue commands called tasks, which are represented by the left-hand column of the data base. For example, a user may want to calculate the stresses in a supersonic flight condition. He "punches" Loads and Structural Analysis. From the computer programs represented by the center column of the data base, the computer picks out the appropriate programs - a supersonic aerodynamic program and a structural analysis program. From the right-hand column of the data base, the computer gets the configuration data for the vehicle selected. The problem is worked, and the results are returned to the user.

The integration of a system of engineering programs on NOS is described in reference 5. Information on the computational capabilities of the ISSYS program are given in reference 6. The overall sizing activity is discussed in references 3, 7, and 8.

Example application.- An example of results that can be obtained with ISSYS is shown in figure 4. These results are for the wing of a low-aspect-ratio supersonic aircraft similar to that shown in figure 1. In this example, only the face sheets of the honeycomb core sandwich panels on the wing surface are being sized. The dimensions of the core, webs, and spar caps remain constant. All titanium wings and combinations of titanium and graphite-polyimide are considered.

The bar at the far left in figure 4 indicates the wing mass for an all-titanium design. The strength design is about 6000 kg; the flutter fix increases the mass to about 6600 kg. The second bar from the left indicates the wing mass for a wing with graphite-polyimide face sheets on the honeycomb core sandwich panels. The remainder of the wing is titanium. The metal-composite strength design is about 4800 kg. Although the flutter fix is larger for the metal-composite design than for the all-metal design, the total mass (5700 kg) of the metal-composite design is about 14 percent less than that of the all-metal design. The remaining two bars show the effect of changing wing area.

Although only wing structure is represented in figure 4, the full structural model shown in figure 1 is used in the analyses. The full model is particularly important for a valid flutter analysis.

Computer resources are also shown in figure 4. Considering the level of structural detail, we feel that the work is being done in a reasonable time and at a very reasonable cost.

Structural Subassembly Sizing

In the overall vehicle sizing activity which was discussed in the previous section, the goal of considering all the various design requirements simultaneously has not yet been met, and improvements are needed in the sizing approach. In the second area, structural subassembly sizing, all of the newest structural sizing technology is incorporated. The problems, however, are smaller - on the order of one-half to one-tenth the size of the overall vehicle sizing problem. In the overall vehicle work, a system of computer programs is used. In the structural subassembly work, a single stand-alone computer program is generally used.

<u>Approach</u>.- As in the overall vehicle work, the structural subassembly sizing work is based on finite-element structural models. A simplified sketch of a finite-element model of a wing structure is shown in figure 5. Many types of inequality constraints have been considered. Deflection and twist constraints, for example, mean that under the design load the deflection and twist of the wing tip must be less than some specified value.

Because the structural subassembly sizing work uses rigorous sizing approaches, numerous constraints, and complex finite-element models, we have developed new techniques to improve computational efficiency. Some of these techniques are listed in figure 5. Approximate analyses are updated periodically to insure a correct solution. Constraint deletion simply means ignoring unimportant constraints. Design variable linking refers to reducing the number of independent sizing variables involved in the computations. Finally, we have made substantial improvements to the basic math programming search techniques that are used in all the subassembly sizing work. Techniques for improving computational efficiency and studies exploring the introduction of various constraints are presented in references 9 to 22.

<u>Example application</u>.- A high-aspect-ratio subsonic wing box made of graphite-epoxy (fig. 6) is sized for minimum mass and subject to design constraints on material strength, deflection and twist of the wing tip, and

buckling of the wing cover panels. The sizing variables are the thickness of wing cover panels, the thickness of spar webs, and the areas of spar caps. The wing box, shown in figure 6, is divided into seven spanwise segments. Two types of sizing variable distributions are considered - (1) a coarse distribution in which the sizing variables are uniform within a spanwise segment and (2) a refined distribution in which the sizing variables have a chordwise variation within the spanwise segment. In the first case, the wing box has only a spanwise variation in the sizing variables. In the second case, the wing box has a chordwise as well as a spanwise variation in the sizing variables. In this exercise, the sizing variable distribution, not the finite-element model, is being refined between case 1 and case 2.

Results are presented in figures 7 and 8. The final chordwise variations in the wing cover skin in segment 4 (fig. 6) are shown in figure 7 for both the coarse and refined distributions. In each sketch, LE and TE stand for leading and trailing edges, respectively, of the wing box. Because a composite material is being used for the wing skins, it is possible to vary the proportions at the different orientations. As expected, in the refined sizing variable distribution case, the 0° filaments, which are spanwise, are concentrated at the trailing edge of this sweptback wing box.

The effect on mass is shown in figure 8. Again, as would be expected, a chordwise variation in material can save weight - in this case, about 15 percent. The computer resources are reasonable.

This example is taken from reference 9. From the point of view of sizing methodology, the studies in reference 9 mark the first time wing panel buckling has been treated properly for an entire wing structure. The procedure takes advantage of the capability to favorably influence load paths.

Thermal Structures

The third structural sizing activity involves thermal structures. This work is aimed at developing the special techniques that might be needed for sizing high-speed aircraft and space vehicles for which temperatures and thermal stresses could become important design considerations. Research in this area is described in references 23 to 28.

Problem characteristics.- The general thermal design problem characterized in figure 9 may involve both thermal and mechanical loads that vary with time so that both steady-state and time-dependent analyses may be required. The temperatures and stresses must be controlled simultaneously. The goal is to trade the mass of the thermal control system, such as insulation, against structural mass to obtain a low-mass total system.

Example.- An example of a steady-state thermal sizing problem is presented in figure 10. The example demonstrates the value of a simple, recently developed sizing procedure denoted thermal fully stressed design (TFSD). It is very similar to fully stressed design (FSD) with stress ratio sizing. In the case of bar elements, sizing formulas for FSD and TFSD are given by the following equations:

(For FSD) $$A_{i+1} = \left(\frac{\sigma_{Mi} + \sigma_{Ti}}{\sigma_a}\right) A_i$$

(For TFSD) $$A_{i+1} = \left(\frac{\sigma_{Mi}}{\sigma_a - \sigma_{Ti}}\right) A_i$$

in which A is the area of the bar element, i is the iteration number, σ_M is the stress due to mechanical loads, σ_T is the stress due to thermal loads, and σ_a is the allowable stress. The same basic approach is used to obtain the sizing formula for membrane elements. The procedure is explained in detail in reference 23.

The sketch at the left in figure 10 gives the results of convergence studies carried out using FSD and TFSD. The sketch shows the trend in the number of cycles required for convergence of each sizing procedure as a function of the temperature, or thermal stress, of the structure. Both procedures diverge for very high thermal stresses. Experience with several thermal sizing problems indicates that in the temperature range where thermal stresses are moderate, TFSD converges two to four times as fast as regular fully stressed design (refs. 23 to 25). These convergence studies were made with fairly simple models such as the one at the right in figure 10. It is believed, however, that the approach is applicable to more complex models.

It is known that FSD provides minimum-mass designs for structures that are statically determinate.[1] Satisfactory results are usually obtained for structures that are nearly statically determinate and for structures whose sizing variables have only a small effect on internal load distribution. According to reference 25, FSD and TFSD converge to the same design. Because of superior convergence characteristics for thermally stressed structures, TFSD is recommended over FSD in thermal design problems. But there are structural sizing problems for which the final designs provided by both FSD and TFSD are not the minimum-mass designs. For these types of problems, rigorous methods such as mathematical programming and rigorous optimality criteria must be employed. These rigorous methods are also being studied in our thermal sizing activities (ref. 23).

Stiffened Panels

The fourth and final area of sizing activity is stiffened panels. As was stated earlier in this paper, Langley has a strong analytical and experimental program aimed at the design of efficient stiffened composite panels. This research program has produced numerous technical reports (refs. 29 to 40)

---

[1] It is of interest to recall that thermal stresses do not exist for statically determinate structures.

dealing with both analytical and experimental aspects of the program. (Reference 40 is included because it is closely related to the work at Langley.) The present report focuses on the latest stiffened panel sizing code developed under this research program. The code, denoted PASCO (Panel Analysis and Sizing COde), will be available through COSMIC.

Description and capabilities.- Some of the important capabilities of the code are indicated in figure 11. The panel may be loaded by any combination of in-plane loadings (tension, compression, and shear) and lateral pressure. The code includes a rigorous buckling analysis that can account for complex buckling modes of arbitrary panel configurations. The panel cross section is assumed to be an assembly of plate elements, with each plate element consisting of a balanced symmetric laminate of any number of layers. The code can also be used to size metal panels. Stresses caused by a bow-type initial imperfection or lateral pressure are accounted for by using a beam-column approach. A more complete discussion of the code is presented in reference 29.

Examples.- The examples considered in this paper are for blade-stiffened panels having the configuration shown in figure 12. The sizing variables are the element widths B_i and the lamina thicknesses T_j. In this example, 0° filaments are placed in the center and $\pm 45^{\circ}$ filaments are placed on either side.

The first results, which are presented in figure 13, are for aluminum blade-stiffened panels and graphite-epoxy blade-stiffened panels. The data are presented in the form of a structural efficiency diagram in which the mass index $\frac{W/A}{L}$ (weight per unit area divided by the panel length) is plotted as a function of the loading index N_x/L (longitudinal loading divided by the panel length). Both scales are logarithmic. In a typical aircraft wing structure, the lightly loaded panels near the tip might have a loading index on the order of 700 kPa. The heavily loaded panels at the root might have a loading index of 5000 kPa. In this example, the only constraint considered is buckling. According to figure 13, the aluminum panels weigh about twice as much as graphite-epoxy panels.

But would these panels of figure 13 carry the design load? The answer is that they probably would not. These data are for perfect panels, but real panels are not perfect. There are geometric imperfections that can greatly reduce the buckling load. There are also other design requirements that must be taken into account in order for the design to be practical. The sizing code can account for several of these practical design requirements, including an overall bow-type imperfection.

A panel with an initial bow is shown in figure 14. The magnitude of the eccentricity at the center is denoted e. The bow can be positive or negative. The quantity e/L is an important nondimensional parameter that is useful in scaling designs.

The first-order effect of the bow is assumed to be the additional stresses produced by bending. These additional stresses affect the local buckling load and the loading at which material strength considerations become important. At the center of the panel, the bending moment is largest and is given by

$$M = \frac{N_x e}{1 - \frac{N_x}{N_{x_E}}}$$

in which N_x is the applied axial load per unit width and N_{x_E} is the Euler buckling load for the panel.

The effect of a bow on the buckling load of a panel designed for zero bow is shown in figure 15. For a panel of length 76 cm (30 in.), a bow of only 0.25 cm (0.1 in.) causes a reduction in the buckling load of about 35 percent. In general, this imperfection curve is not symmetric.

The increase in panel mass caused by accounting for practical design considerations such as an overall bow is shown in figure 16. This structural efficiency diagram is for graphite-epoxy blade-stiffened panels only. As shown in the legend, the solid lines are for buckling only. The dashed curves have an additional requirement that the strains not exceed ± 0.004. Imposing a limitation of 0.004 is an attempt to account for the possible presence of cracks, flaws, delaminations, and impact damage. Some evidence suggests that 0.004 may be too large a number.

The lowest curve in figure 16 is for buckling of perfect panels. It is the same as the graphite-epoxy curve in figure 13. The next higher curve is for buckling of panels with an initial bow of $e/L = \pm 0.003$. The positive and negative sign means that these panels carry the load whether the bow is positive or negative. The curve with long dashes that merges with the solid line shows the effect of adding the strain limitation to the buckling requirement.

The highest curve, which is made up of short dashes, shows the effect of adding shear and extensional stiffness requirements that are typical of aircraft wing panels. In other words, these panels account for stiffness, buckling, overall bow-type imperfections, and have an allowable strain requirement. All of these factors influence the curve. Run times are reasonable, on the order of 2 to 5 min.

CONCLUDING REMARKS

In summary, there are aircraft structural design challenges caused by new and unusual aircraft configurations, new materials, and new technologies such as active controls. In this paper, it is suggested that computerized sizing techniques could help meet some of these design challenges.

There are basically four areas of structural sizing research underway at Langley Research Center. With respect to overall vehicle work, a prototype version of the structural sizing system has been made operational. With respect to subassembly work, the most advanced sizing techniques have been incorporated in our stand-alone computer programs. In thermal structures, the time-dependent thermal effects problem is now being attacked. And, finally, an advanced stiffened panel sizing code has been developed and will be made available through COSMIC.

REFERENCES

1. Nagel, A. L.: Studies of Advanced Transport Aircraft. CTOL Transport Technology - 1978, NASA CP-2036, Pt. II, 1978, pp. 951-982.

2. Heldenfels, Richard R.: Automating the Design Process: Progress, Problems, Prospects, Potential. AIAA Paper No. 73-410, Mar. 1973.

3. Sobieszczanski, Jaroslaw; McCullers, L. Arnold; Ricketts, Rodney H.; Santoro, Nick J.; Beskenis, Sharon D.; and Kurtze, William L.: Structural Design Studies of a Supersonic Cruise Arrow Wing Configuration. Proceedings of the SCAR Conference - Part 2, NASA CP-001, [1977], pp. 659-683.

4. Ricketts, Rodney H.; and Sobieszczanski, Jaroslaw: Simplified and Refined Structural Modeling for Economical Flutter Analysis and Design. Volume B - Dynamics, Structural Dynamics, AIAA/ASME 18th Structures, Structural Dynamics & Materials Conference, Mar. 1977, pp. 117-126.

5. Sobieszczanski, Jaroslaw: Building a Computer-Aided Design Capability Using a Standard Time Share Operating System. Integrated Design and Analysis of Aerospace Structures, R. F. Hartung, ed., American Soc. Mech. Eng., 1975, pp. 93-112.

6. Giles, Gary L.: Computer-Aided Methods for Analysis and Synthesis of Supersonic Cruise Aircraft Structures. Proceedings of the SCAR Conference - Part 2, NASA CP-001, [1977], pp. 637-657.

7. Sobieszczanski, Jaroslaw: Sizing of Complex Structure by the Integration of Several Different Optimal Design Algorithms. Paper presented at the AGARD Lecture Series No. 70 on Structural Optimization (Hampton, Virginia), Oct. 1974.

8. Giles, Gary L.; and McCullers, L. A.: Simultaneous Calculation of Aircraft Design Loads and Structural Member Sizes. AIAA Paper No. 75-965, Aug. 1975.

9. Starnes, James H., Jr.; and Haftka, Raphael T.: Preliminary Design of Composite Wings for Buckling, Strength and Displacement Constraints. A Collection of Technical Papers - AIAA/ASME 19th Structures, Structural Dynamics and Materials Conference, Apr. 1978, pp. 1-13. (Available as AIAA Paper No. 78-466.)

10. Schmit, L. A., Jr.; and Farshi, B.: Some Approximation Concepts for Structural Synthesis. AIAA J., vol. 12, no. 5, May 1974, pp. 692-699.

11. Schmit, Lucien A., Jr.; and Miura, Hirokazu: Approximation Concepts for Efficient Structural Synthesis. NASA CR-2552, 1976.

12. Haftka, Raphael T.: Automated Procedure for Design of Wing Structures to Satisfy Strength and Flutter Requirements. NASA TN D-7264, 1973.

13. Haftka, Raphael T.; and Starnes, James H., Jr.: WIDOWAC (Wing Design Optimization With Aeroelastic Constraints): Program Manual. NASA TM X-3071, 1974.

14. Schmit, L. A,; and Miura, H.: A New Structural Analysis/Synthesis Capability - ACCESS 1. AIAA J., vol. 14, no. 5, May 1976, pp. 661-671.

15. Schmit, L. A.; and Miura, H.: An Advanced Structural Analysis/Synthesis Capability - ACCESS 2. Int. J. Num. Methods Eng., vol. 12, no. 2, 1978, pp. 353-377.

16. Haftka, Raphael T.: Parametric Constraints With Application to Optimization for Flutter Using a Continuous Flutter Constraint. AIAA J., vo. 13, no. 4, Apr. 1975, pp. 471-475.

17. Haftka, Raphael T.; and Starnes, James H., Jr.: Applications of a Quadratic Extended Interior Penalty Function for Structural Optimization. AIAA J., vol. 14, no. 6, June 1976, pp. 718-724.

18. Miura, Hirokazu; and Schmit, Lucien A., Jr.: ACCESS-1: Approximation Concepts Code for Efficient Structural Synthesis - Program Documentation and User's Guide. NASA CR-144905, 1976.

19. Haftka, Raphael T.; and Yates, E. Carson, Jr.: Repetitive Flutter Calculations in Structural Design. J. Aircr., vol. 13, no. 7, July 1976, pp. 454-461.

20. Haftka, Raphael T.; Starnes, James H., Jr.; Barton, Furman W.; and Dixon, Sidney C.: Comparison of Two Types of Structural Optimization Procedures for Flutter Requirements. AIAA J., vol. 13, no. 10, Oct. 1975, pp. 1333-1339.

21. Stroud, W. Jefferson: Automated Structural Design With Aeroelastic Constraints: A Review and Assessment of the State of the Art. Structural Optimization Symposium, L. A. Schmit, Jr., ed., AMD-Vol. 7, American Soc. Mech. Eng., c. 1974, pp. 77-118.

22. Haftka, Raphael T.: Optimization of Flexible Wing Structures Subject to Strength and Induced Drag Constraints. AIAA J., vol. 15, no. 8, Aug. 1977, pp. 1101-1106.

23. Adelman, Howard M.; Sawyer, Patricia L.; and Shore, Charles P.: Development of Methodology for Optimum Design of Structures at Elevated Temperatures. A Collection of Technical Papers - AIAA/ASME 19th Structures, Structural Dynamics and Materials Conference, Apr. 1978, pp. 23-36. (Available as AIAA Paper No. 78-468.)

24. Adelman, Howard M.; Walsh, Joanne L.; and Narayanaswami, R.: An Improved Method for Optimum Design of Mechanically and Thermally Loaded Structures. NASA TN D-7965, 1975.

25. Adelman, Howard M.; and Narayanaswami, R.: Resizing Procedure for Structures Under Combined Mechanical and Thermal Loading. AIAA J., vol. 14, no. 10, Oct. 1976, pp. 1484-1486.

26. Rao, G. Venkateswara; Shore, Charles P.; and Narayanaswami, R.: An Optimality Criterion for Sizing Members of Heated Structures With Temperature Constraints. NASA TN D-8525, 1977.

27. Adelman, Howard M.; and Sawyer, Patricia L.: Inclusion of Explicit Thermal Requirements in Optimum Structural Design. NASA TM X-74017, 1977.

28. Adelman, Howard M.; and Narayanaswami, R.: Resizing Procedure for Optimum Design of Structures Under Combined Mechanical and Thermal Loading. NASA TM X-72816, 1976.

29. Anderson, Melvin S.; and Stroud, W. Jefferson: A General Panel Sizing Computer Code and Its Application to Composite Structural Panels. A Collection of Technical Papers - AIAA/ASME 19th Structures, Structural Dynamics and Materials Conference, Apr. 1978, pp. 14-22. (Available as AIAA Paper No. 78-467.)

30. Stroud, W. Jefferson; Anderson, Melvin S.; and Hennessy, Katherine W.: Effect of Bow-Type Initial Imperfection on the Buckling Load and Mass of Graphite-Epoxy Blade-Stiffened Panels. NASA TM-74063, 1977.

31. Stroud, W. Jefferson; Agranoff, Nancy; and Anderson, Melvin S.: Minimum-Mass Design of Filamentary Composite Panels Under Combined Loads: Design Procedure Based on a Rigorous Buckling Analysis. NASA TN D-8417, 1977.

32. Anderson, Melvin S.; Hennessy, Katherine W.; and Heard, Walter L., Jr.: Addendum to Users Guide to VIPASA (Vibration and Instability of Plate Assemblies Including Shear and Anisotropy). NASA TM X-73914, 1976.

33. Stroud, W. Jefferson; and Agranoff, Nancy: Minimum-Mass Design of Filamentary Composite Panels Under Combined Loads: Design Procedure Based on Simplified Buckling Equations. NASA TN D-8257, 1976.

34. Rhodes, Marvin D.; Williams, Jerry G.; and Starnes, James H., Jr.: Effect of Impact Damage on the Compression Strength of Filamentary-Composite Hat-Stiffened Panels. Presented at the 23rd SAMPE National Symposium and Exhibition (Anaheim, Calif.), May 2-4, 1978.

35. Rhodes, Marvin D.; Williams, Jerry G.; and Starnes, James H., Jr.: Effect of Low-Velocity Impact Damage on the Compressive Strength of Graphite-Epoxy Hat-Stiffened Panels. NASA TN D-8411, 1977.

36. Mikulas, Martin M., Jr.; Bush, Harold G.; and Rhodes, Marvin D.: Current Langley Research Center Studies on Buckling and Low-Velocity Impact of Composite Panels. Third Conference on Fibrous Composites in Flight Vehicle Design, Part II, NASA TM X-3377, 1976, pp. 633-663.

37. Williams, Jerry G.; and Stein, Manuel: Buckling Behavior and Structural Efficiency of Open-Section Stiffened Composite Compression Panels. AIAA J., vol. 14, no. 11, Nov. 1976, pp. 1618-1626.

38. Williams, Jerry G.; and Mikulas, Martin M., Jr.: Analytical and Experimental Study of Structurally Efficient Composite Hat-Stiffened Panels Loaded in Axial Compression. NASA TM X-72813, 1976. (Also available as AIAA Paper No. 75-754.)

39. Agarwal, Banarsi; and Davis, Randall C.: Minimum-Weight Designs for Hat-Stiffened Composite Panels Under Uniaxial Compression. NASA TN D-7779, 1974.

40. Purdy, D. M.; and Dietz, C. G.: Optimum Design of Composite Primary Structure Aircraft Components. ICAS Paper No. 76-07, Oct. 1976.

DESIRED OUTPUT

- STATIC AND DYNAMIC AEROELASTIC CHARACTERISTICS WITH AND WITHOUT ACTIVE CONTROLS
- STRUCTURAL MASS AND STIFFNESS DISTRIBUTION
- STRUCTURAL LAYOUT AND DIMENSIONS OF KEY STRUCTURAL MEMBERS

TYPICAL FINITE-ELEMENT MODEL

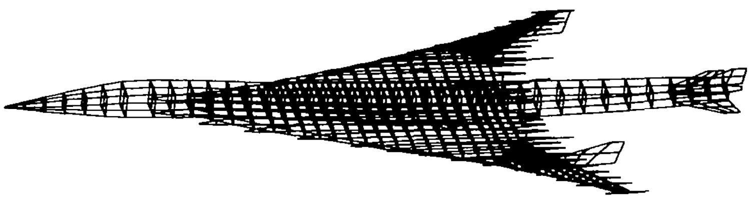

750 GRID POINTS, 2400 ELEMENTS, 720 SIZING VARIABLES

Figure 1.- Overall vehicle structural sizing.

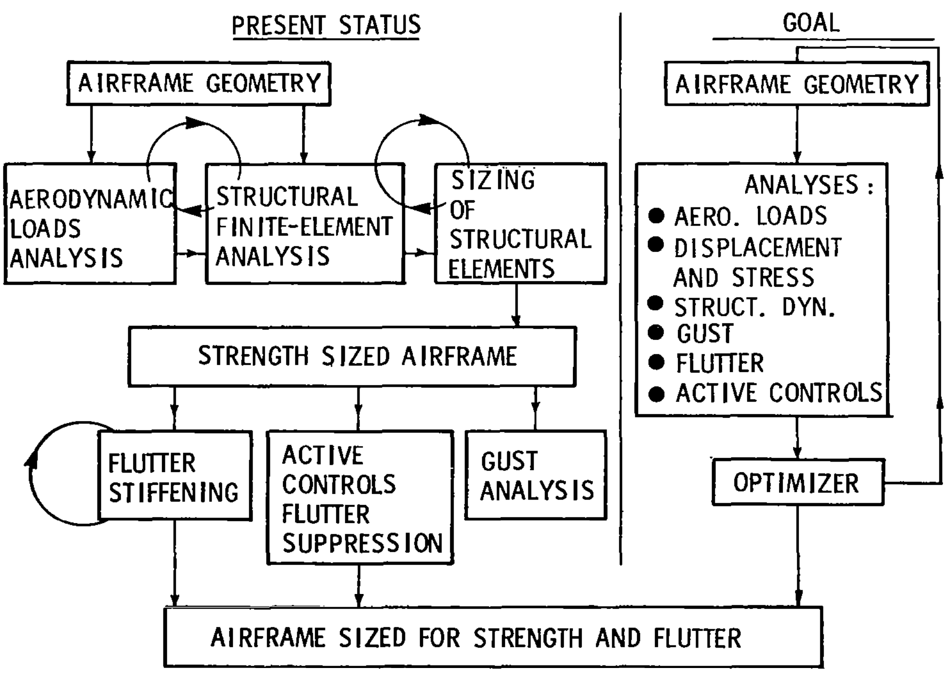

Figure 2.- Airframe structural sizing approach.

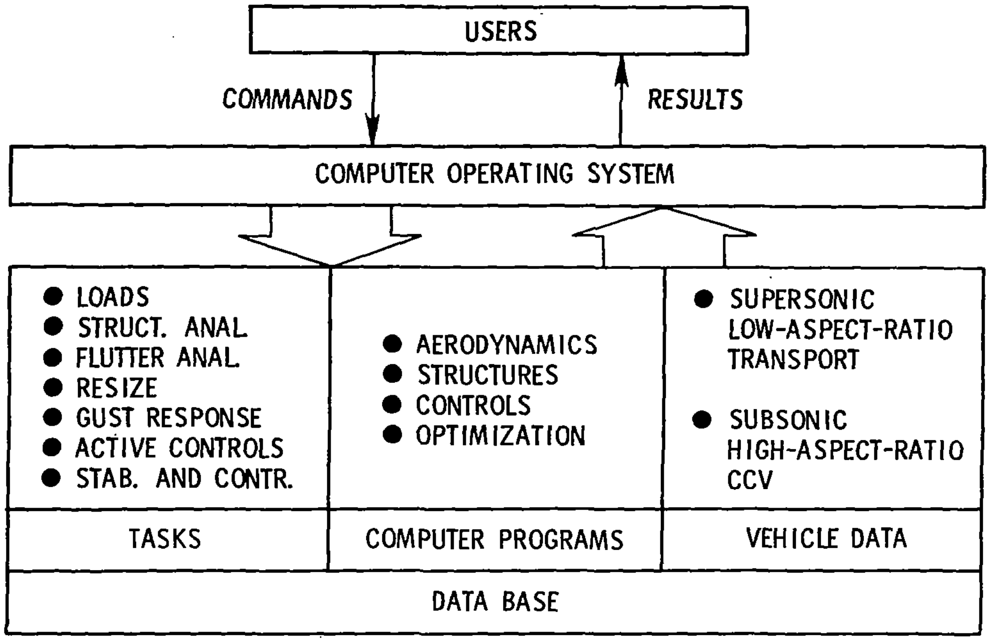

Figure 3.- Integrated multidisciplinary sizing system.

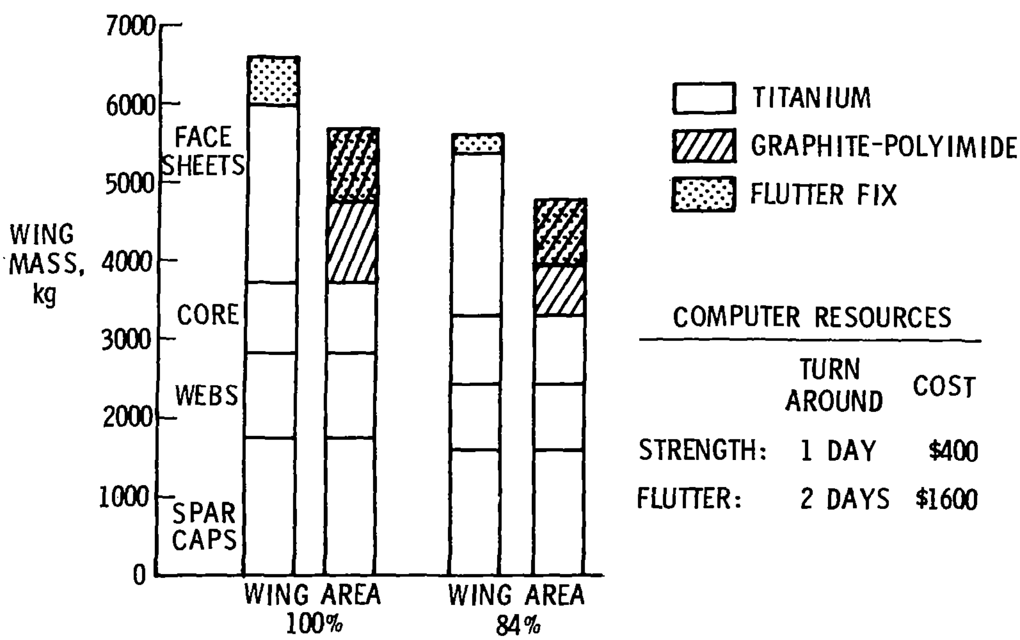

Figure 4.- Mass of optimally sized low-aspect-ratio wings.

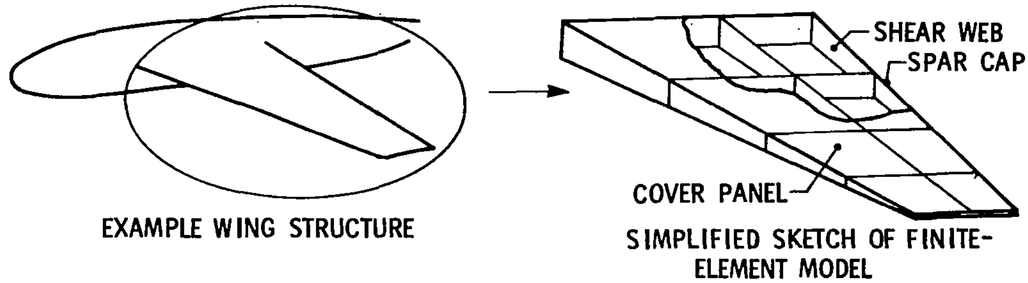

- CONSTRAINTS CONSIDERED

MATERIAL STRENGTH	BUCKLING
DEFLECTION	NATURAL FREQUENCY
TWIST	FLUTTER
THERMAL STRESS	DRAG

- ADVANCES IN TECHNIQUE

APPROXIMATE ANALYSIS	DESIGN VARIABLE LINKING
CONSTRAINT DELETION	IMPROVED SEARCH TECHNIQUES

Figure 5.-Structural subassembly sizing.

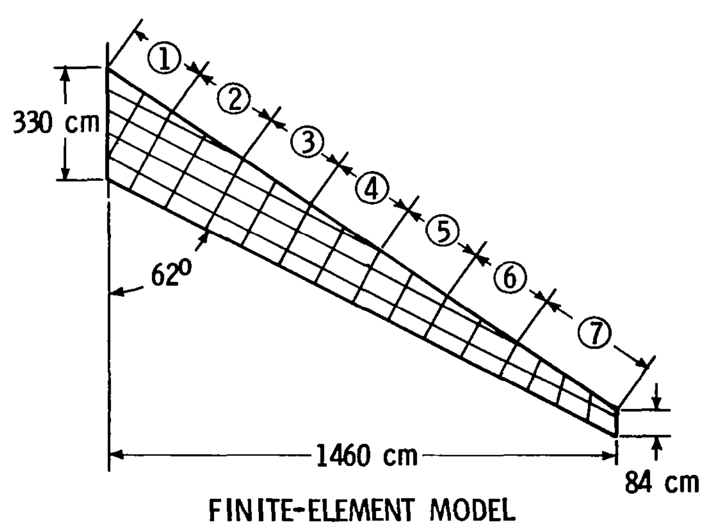

Figure 6.- Application of subassembly sizing for a graphite-epoxy wing structure with material strength, displacement, and buckling constraints.

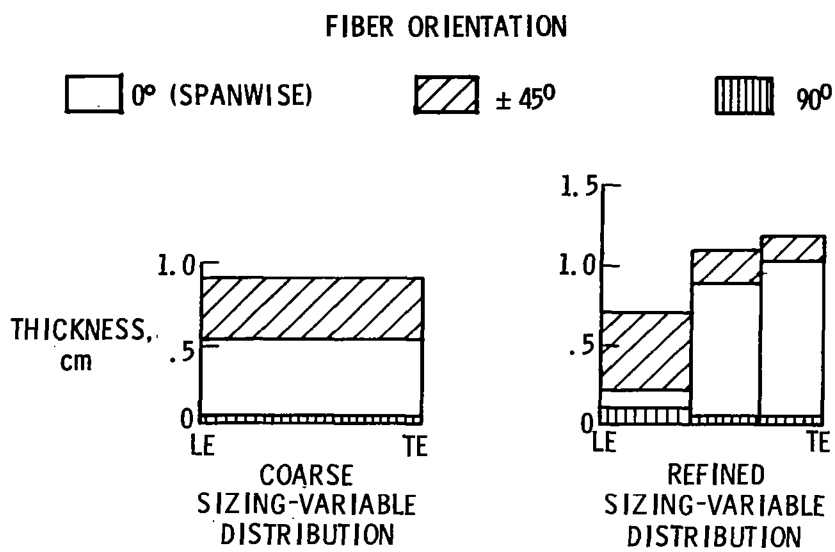

Figure 7.- Cover skin thickness distribution at 40 percent of semispan.

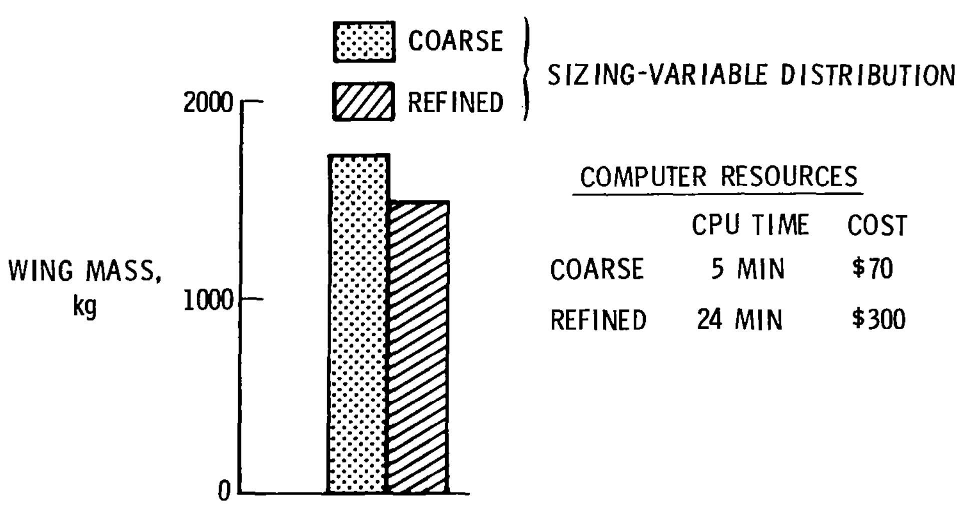

Figure 8.- Mass of optimally sized high-aspect-ratio wing.

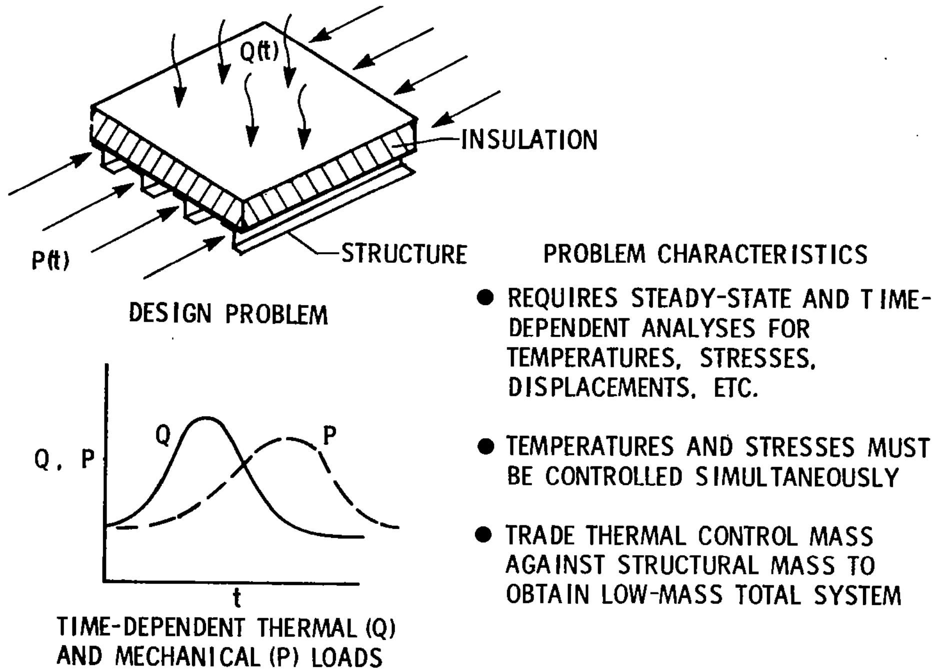

Figure 9.- Sizing thermal structures.

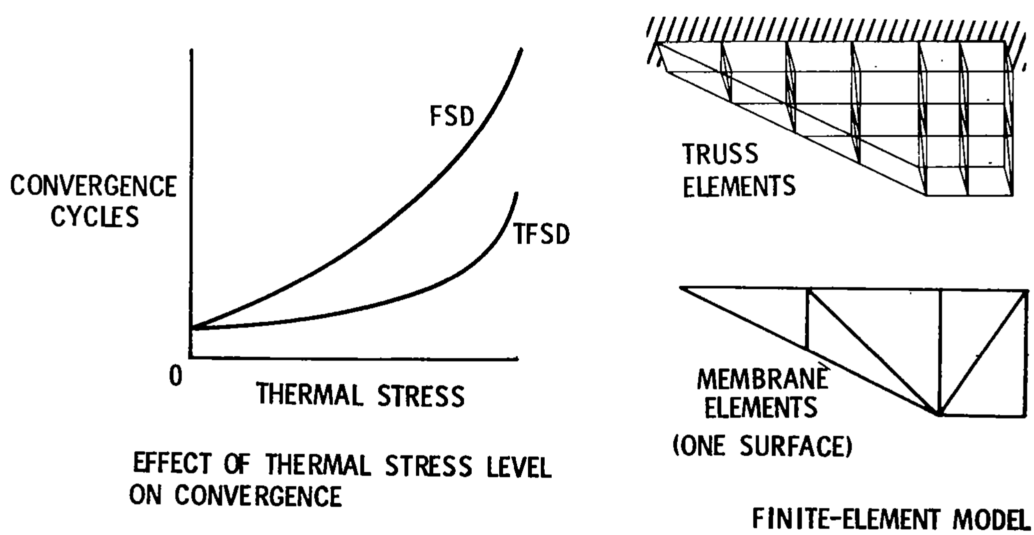

Figure 10.- Example using thermal fully stressed design procedure for a low-aspect-ratio wing with fixed applied loads and temperatures.

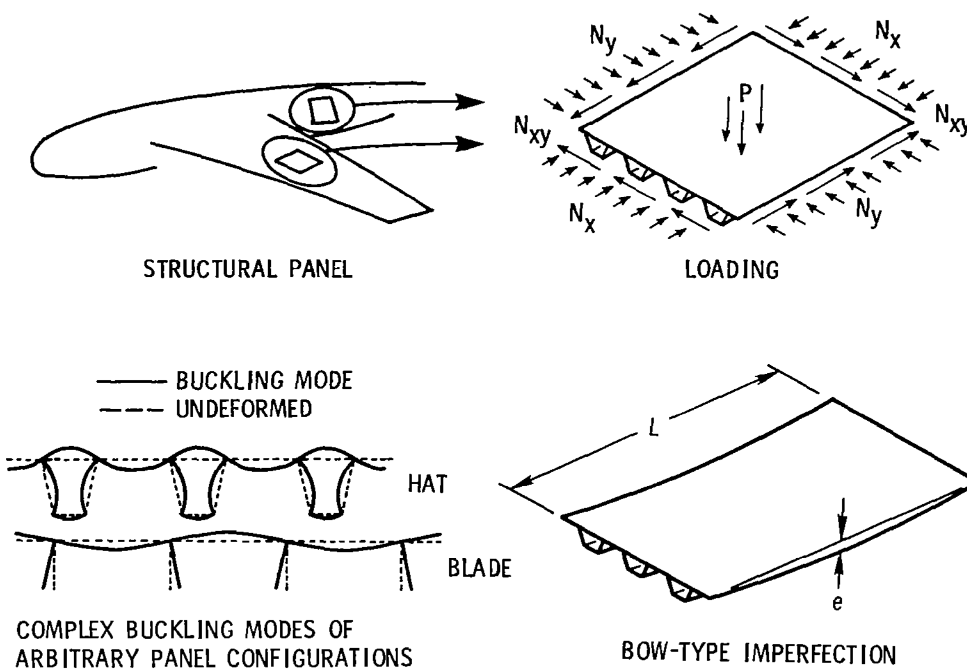

Figure 11.- Stiffened panel design code - PASCO. (N_x and N_y are the longitudinal and transverse in-plane loadings, respectively, N_{xy} is the shear landing, and P is the pressure loading.)

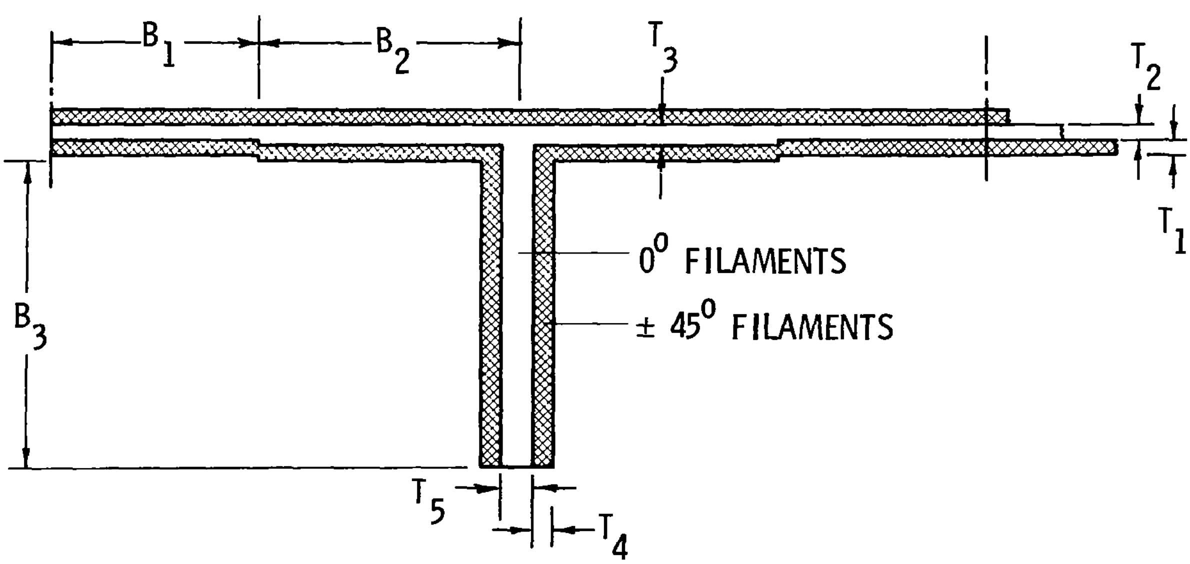

Figure 12.- Sizing variables for composite blade-stiffened panel.

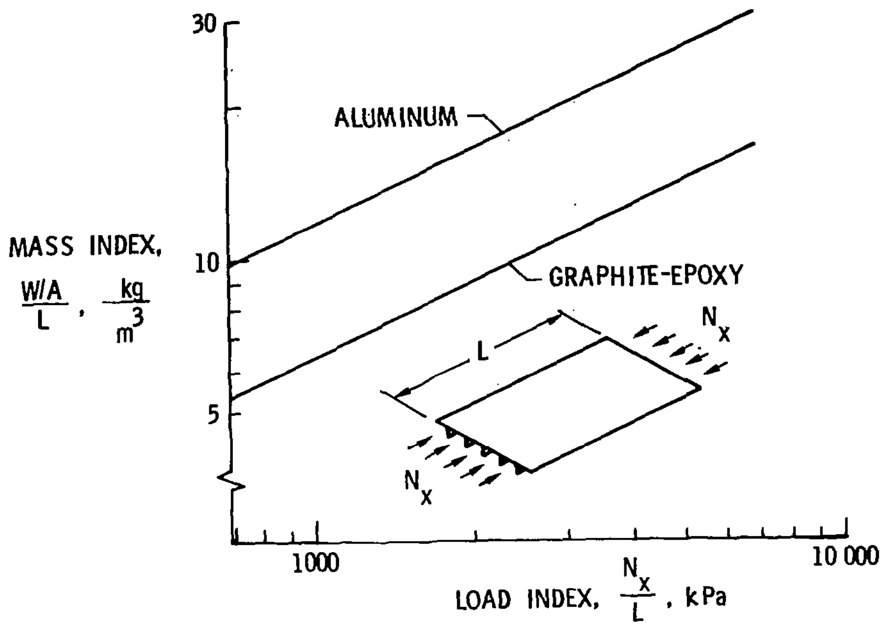

Figure 13.- Structural efficiency of blade-stiffened panels (only buckling considered).

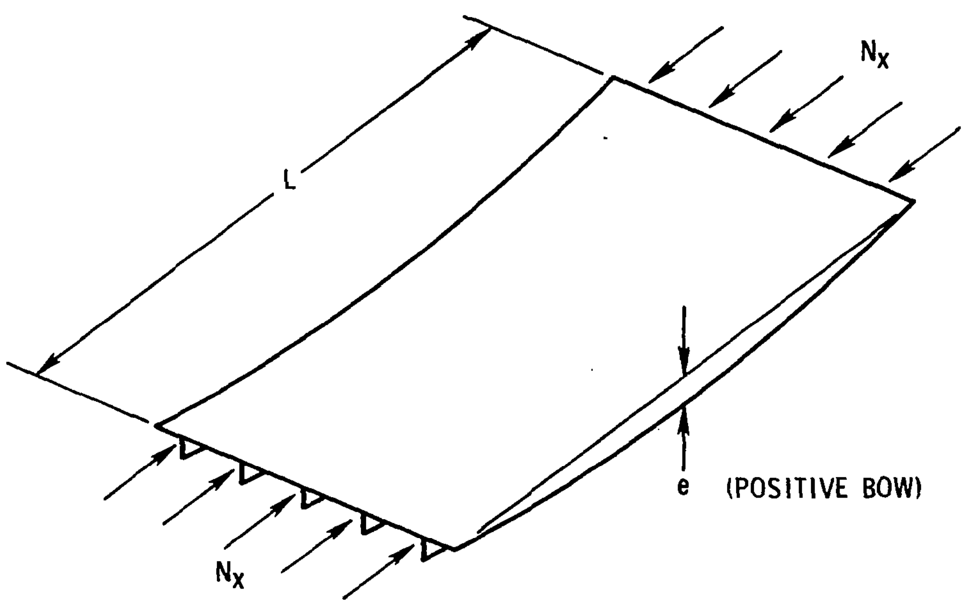

Figure 14.- Panel with initial bow.

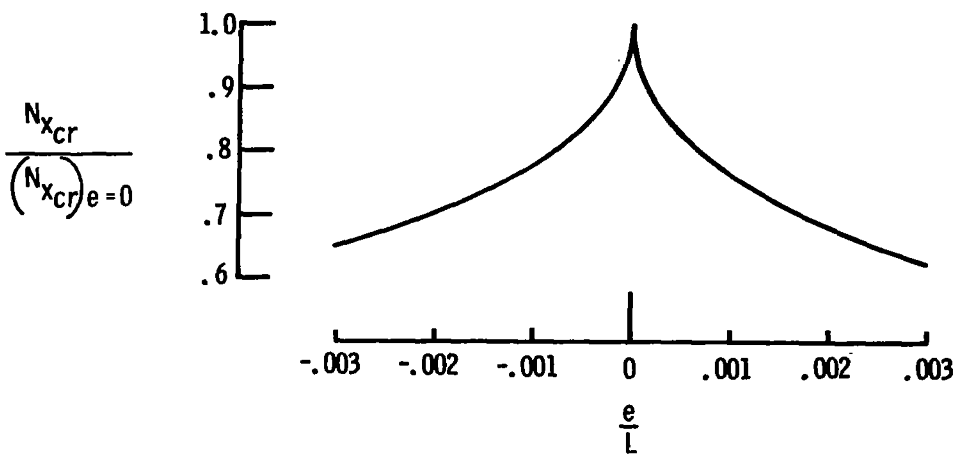

Figure 15.- Effect of bow on buckling load. (Ratio of buckling load $N_{x_{cr}}$ for panel with a bow to buckling load of panel without a bow $(N_{x_{cr}})_{e=0}$ as a function of size of bow e/L for graphite-epoxy, blade-stiffened panel designed for zero bow.)

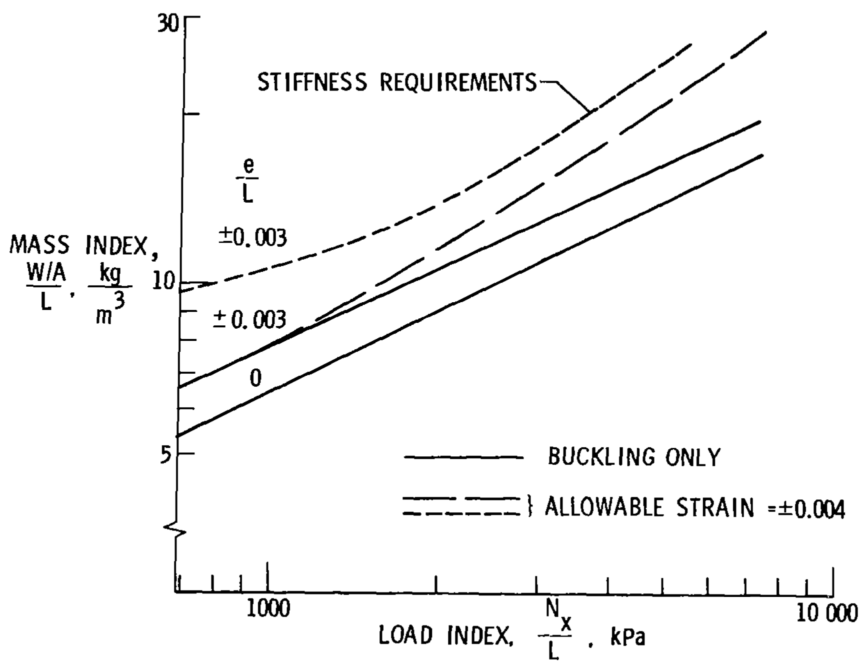

Figure 16.- Structural efficiency of graphite-epoxy, blade-stiffened panels.